sustainability

MDPI

Article

Impacts of Bedrocks on Vegetation Carbons in Typical Karst Areas: A Case Study in Puding County, Southwest China

Xianli Cai [1,2,3], Weijun Luo [1,2,*], Changcheng Liu [4], Jia Chen [1,2], Lin Zhang [1,2,3], Anyun Cheng [1,2], Zhongquan He [5] and Shijie Wang [1,2]

[1] State Key Laboratory of Environmental Geochemistry, Institute of Geochemistry, Chinese Academy of Sciences, Guiyang 550081, China; caixianli@mail.gyig.ac.cn (X.C.)
[2] Puding Karst Ecosystem Research Station, Chinese Academy of Sciences, Anshun 562100, China
[3] University of Chinese Academy of Sciences, Beijing 100049, China
[4] State Key Laboratory of Vegetation and Environmental Change, Institute of Botany, Chinese Academy of Sciences, Beijing 100093, China
[5] Organization Department, Qianxinan Buyi and Miao Autonomous Prefecture Committee of the CPC, Xingyi 562400, China
* Correspondence: luoweijun@vip.gyig.ac.cn

Abstract: An accurate estimation of vegetation carbon pools and their carbon sequestration potential is significant in global carbon cycle research but the existing estimations are still insufficient and largely uncertain. Here, we estimated the vegetation carbon density, carbon stocks, and carbon sequestration potential under three main bedrock types (limestone, dolomite, and non-carbonate) in Puding County, Guizhou Province, Southwestern China. The data used here included high-resolution vegetation maps of Puding, data from 274 sample plots, and the carbon contents measured previously in adjacent areas. The land area ratio of natural vegetation at an early stage (namely, grassland and shrub, excluding artificial forests and cultivated land) in carbonate rock areas is significantly larger than that in non-carbonate areas. The average existing carbon densities of vegetation in the non-carbonate, limestone, and dolomite areas were 31.59 ± 7.43, 16.75 ± 4.12, and 8.26 ± 2.45 Mg·ha^{-1}, respectively, while their existing carbon stocks were 752.37 ± 172.85, 855.69 ± 210.65, and 208.49 ± 61.82 Gg, respectively. The maximum vegetation carbon densities of mature forests in the three bedrock types were 156.49 ± 12.92, 130.27 ± 6.05, and 117.41 ± 30.03 Mg·ha^{-1}, respectively. Then, their average vegetation carbon sequestration potentials were 56.07 ± 23.06, 70.13 ± 11.39, and 59.11 ± 33.00 Mg·ha^{-1}, respectively. In other words, vegetation carbon stocks in the non-carbonate, limestone, and dolomite areas increased by 1.34 ± 0.42, 3.58 ± 0.48, and 1.49 ± 0.51 Tg, respectively, after continuous evolution to mature forests. In conclusion, the potential growth of carbon density for karst vegetation is slightly higher than that of non-karst vegetation, despite its lower existing carbon density. Additionally, natural vegetation has a greater potential for carbon sequestration than plantations on all three bedrock types.

Keywords: karst; bedrock types; vegetation carbons; carbon sequestration potential; Puding

check for updates

Citation: Cai, X.; Luo, W.; Liu, C.; Chen, J.; Zhang, L.; Cheng, A.; He, Z.; Wang, S. Impacts of Bedrocks on Vegetation Carbons in Typical Karst Areas: A Case Study in Puding County, Southwest China. *Sustainability* **2024**, *16*, 9429. https://doi.org/10.3390/su16219429

Academic Editor: Anna De Marco

Received: 30 September 2024
Revised: 23 October 2024
Accepted: 28 October 2024
Published: 30 October 2024

Copyright: © 2024 by the authors. Licensee MDPI, Basel, Switzerland. This article is an open access article distributed under the terms and conditions of the Creative Commons Attribution (CC BY) license (https://creativecommons.org/licenses/by/4.0/).

1. Introduction

The Paris Agreement was proposed in 2015 to reduce greenhouse gas emissions and mitigate the greenhouse effect. Reducing greenhouse gas emissions and increasing greenhouse gas sequestration are two ways to alleviate the greenhouse effect. Global terrestrial ecosystems can turn about 1/6 of atmospheric CO_2 annually or fix 15–30% of carbon emissions from fossil fuel combustion [1,2]. Vegetation is one major carbon sequester and carbon pool in terrestrial ecosystems [2]. The expansion of vegetation areas and the increase in vegetation carbon density can both enhance vegetation carbon storage [3,4]. As a member of the Paris Agreement, China has actively carried out various emission reduction measures and promoted carbon sequestration through continuous

measures, such as the Grain for Green Project, the Ecological Immigration Project, and comprehensive management of rocky desertification to promote vegetation restoration and increase vegetation carbon sequestration. In 2020, China proposed to achieve the carbon emission peak and carbon neutrality targets by 2030 and 2060, respectively. The annual carbon sink formed by land use change and artificial afforestation in China from 1994 to 2018 ranged from 4.07 to 13.40 Pg [5], indicating the accurate estimation of vegetation carbon sinks is significant for carbon cycle research. However, there is still significant uncertainty in vegetation carbon estimation because of the various research methods used in vegetation carbon research and the inherent ecosystem complexity due to complex influence factors (e.g., the environment and human activities) [6–8].

Bedrocks may impact the overlying vegetation by affecting soil properties and this impact may even obscure and distort climate effects at some scale [9]. Therefore, bedrocks shall be paid attention to in vegetation carbon research. There are about 426,000 km^2 of exposed carbonate rocks in the karst areas of Southwestern China [10]. The ecosystems formed on karst habitats, featured by high calcium/ magnesium contents, high pH, high-porosity bedrocks, and soil deficiency, shall face insufficient water and mineral nutrient supply [11–15]. This harsh environment has a significantly different vegetation species composition and significantly lower net primary productivity compared with non-carbonate-rock areas [16–18]. As reported, the vegetation carbon density of the climax community in Maolan, a typical karst habitat, is about 81.31 $Mg{\cdot}ha^{-1}$ [19]. The aboveground vegetation carbon density of the primary forest in the Houzhai catchment in Southwestern China is about 142.6 $Mg{\cdot}ha^{-1}$ [20] and the carbon density of the secondary forest in the southwestern karst area is 90.9.$Mg{\cdot}ha^{-1}$ [21]. All of these data values are significantly lower than the carbon density of non-karst vegetation in subtropical China (167.4 $Mg{\cdot}ha^{-1}$) [22] and only slightly higher than the average vegetation carbon density of mature forests in China (129.26 $Mg{\cdot}ha^{-1}$) [23]. Nevertheless, studies on NDVI show that the karst region in Southwestern China was a major greening area worldwide in the first two decades of the 21st century [24] and formed a huge vegetation carbon sink thanks to measures such as eco-immigration and ecological engineering [25,26]. However, the problem of how carbonate rocks and non-carbonate rocks affect vegetation carbon characteristics needs further research. There is yet more research on vegetation biomass in the karst areas of Southwestern China but less research on vegetation carbon. Even the existing few studies are based on either small-scale field surveys or remote sensing methods for large-scale estimation [20,21,25,26] while research on vegetation carbon estimation based on a larger-scale field survey is insufficient and needs to be supplied. Limestone and dolomite are the two most widely distributed bedrock types in the karst areas of Southwestern China. The soil weathering from the two bedrocks is significantly different in soil amount and distribution due to the differences in their physical and chemical properties. Soil from dolomite is thin and uniform while soil from limestone is thick and distributed in a patch pattern [27]. How these differences affect vegetation growth and lead to differences in vegetation carbon accumulation needs to be studied.

This study aimed to elucidate the impact of bedrocks on vegetation carbon storage and its sequestration potential in the karst habitats in Southwestern China using a high-resolution vegetation type map and extensive plot surveys. These materials may improve the recognition of the mechanism of karst vegetation carbon sequestration and help propose an appropriate way to study carbon sinks in karst areas.

2. Materials and Methods

2.1. Study Region

This study was carried out in Puding County, Guizhou Province, Southwestern China (105°27′49″–105°58′51″ E, 26°09′36″–26°31′42″ N) (Figure 1). Puding has an altitude from 1042 to 1846 m and a total land area of 1092 km^2. It is located in a subtropical monsoon climate zone with an annual precipitation of 1390 mm and a temperature of 15.1 °C on average. Most precipitations in Puding occur from May to October. Karst in Puding

accounts for 76.73% or 837.93 km^2, including 27.04% or 295.29 km^2 of dolomite and 49.69% or 542.64 km^2 of limestone. Its location in the center of the South China karst region and the relatively comprehensive karst landform types [28] make Puding an ideal place for this study. Yellow soil, as zonal soil in the non-karst areas of this place, is a thicker and even soil layer mainly weathered from basalt rocks. Black limestone soil and yellow limestone soil are the two most widely spread soil types in the karst areas. Black limestone soil with a thinner soil layer, even coverage, and a higher organic matter content, was mainly developed in dolomite areas. In comparison, yellow limestone soil was mainly weathered from limestone and had a patchy thicker soil layer and a lower organic matter content. Both types of soil had higher pH and higher calcium and magnesium contents than zonal yellow soil.

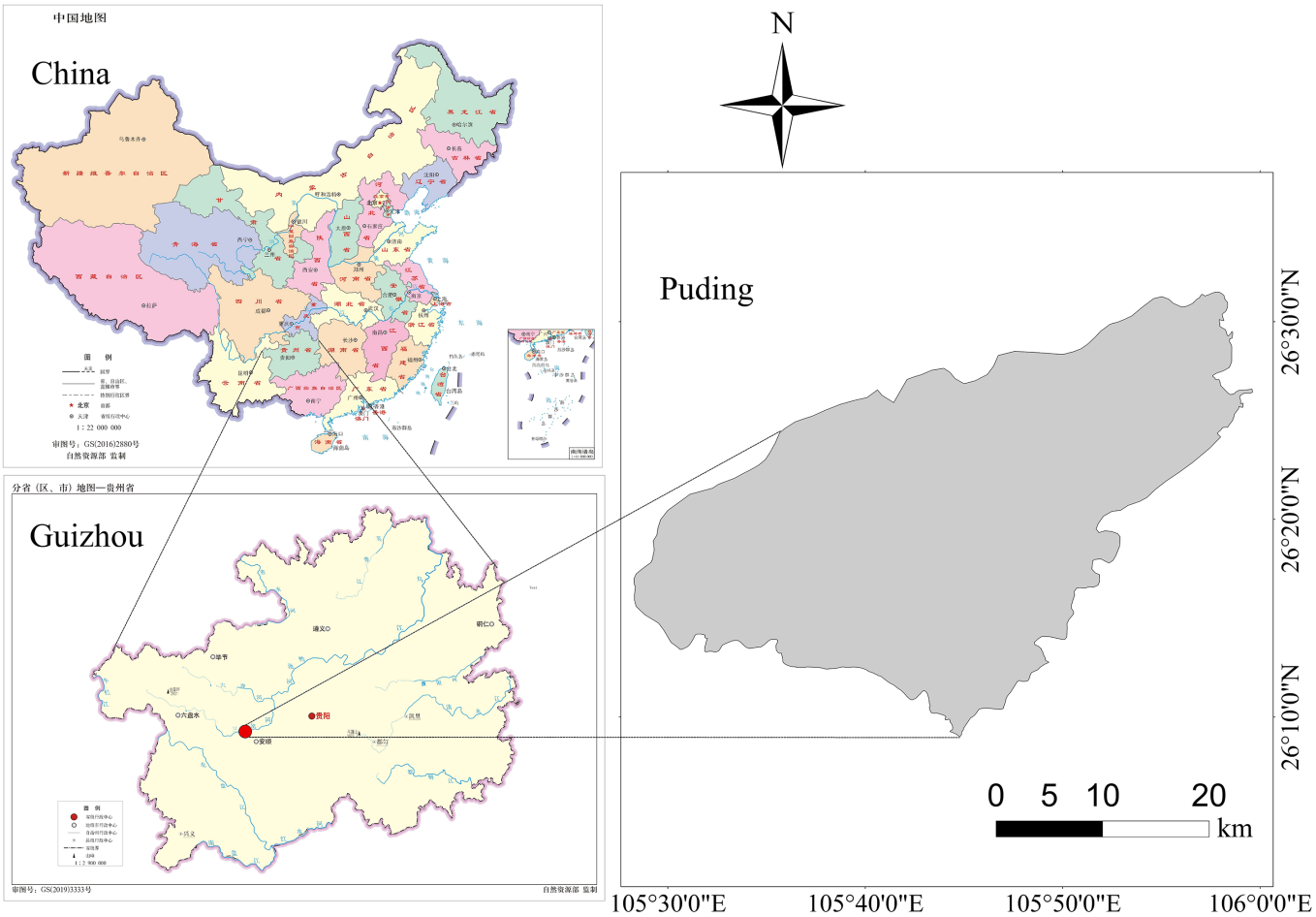


Figure 1. Location of Puding County in Southwest China. The map of China and Guizhou cited by this figure are both derived from http://bzdt.ch.mnr.gov.cn/ with their drawing review numbers of GS(2016)2880 and GS(2019)3333, respectively.

Typical vegetation types in the study area are subtropical evergreen broad-leaved forests on the normal landform and mixed evergreen and deciduous broad-leaved forests in karst habitats. The dominant species in karst forests are *Lithocarpus confinis* and *Platycarya strobilacea*. Puding has nearly no primary forest, but has widespread secondary vegetation and some plantations, because of four instances of thorough vegetation destruction and the Green for Grain Project in the second half of the 20th century. Shrubland and grassland are the two main vegetation types. Plantations account for about 25.6% of non-karst areas, where the main species are *Cunninghamia lanceolata* and *Cryptomeria japonica var. Sinensis*. The most commonly grown species in the plantations of dolomite areas are *Cupressus duclouxiana* and *Cupressus funebris* while the main species grown in the plantations of

limestone areas is *Cryptomeria japonica var. Sinensis*. Agricultural land in Puding is mainly used as paddy fields and dryland. Rapeseed and rice are the main crops in paddy fields while rapeseed and corn are the most commonly planted crops in dryland.

2.2. Drawing and Statistics of the Vegetation–Bedrock Map

Based on the latest high-resolution Google map of Puding in 2019, we first cut the study area into different patches according to color changes. Then, we checked the vegetation types of each patch and adjusted the patch boundaries with on-site inspections during May–September 2019 and May–August 2020 to produce a 1:50,000 vegetation type map of Puding (Figure 2). In this vegetation type map, plantation was subdivided into young plantation and mature plantation while natural vegetation was subdivided into five vegetation types, namely, grassland, shrubland, shrub wood, secondary forest, and mature forest, according to the division system proposed by Yu et al. [29]. Agricultural crops, which were mainly composed of paddy and dryland, were treated as an independent vegetation type from plantation and natural vegetation. After that, a bedrock map of Puding, in which bedrocks were divided into limestone, dolomite, and non-carbonate rock, was overlain onto the vegetation type map to form a vegetation–bedrock map (the attributes of this map is listed in File S2). The area of each vegetation–bedrock type was calculated based on the vegetation–bedrock map. All the work was completed on ArcGIS 10.2.2.

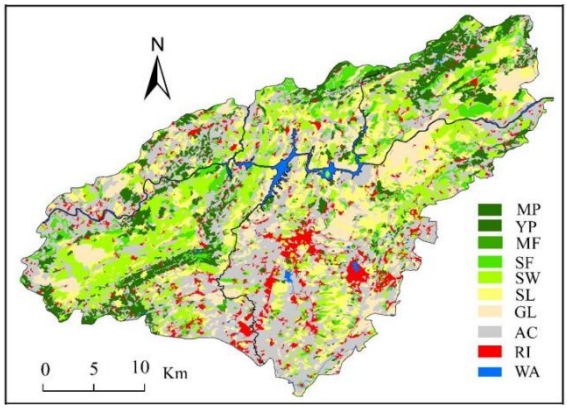


Figure 2. Distribution map of vegetation types in Puding County. MP: mature plantation, YP: young plantation, MF: mature forest, SF: secondary forest, SW: shrub wood, SL: shrubland, GL: grassland, AC: agricultural crop (including PA (paddy) and DL (dryland)), RI: resident inhabitant area, WA: water area.

2.3. Vegetation Survey and Carbon Calculation

2.3.1. Vegetation Survey

Based on the area and distribution pattern of each vegetation–bedrock type (Figure 2), we conducted many survey plots according to the land area and the community complexity of each vegetation–bedrock type. The survey plots on plantations were fewer because of the consistent inter-community growth process while more plots on shrubs and secondary forests were surveyed owing to their complex community structures and large inter-community differences. In total, 266 sample plots were surveyed in Puding. Due to the lack of mature forests in Puding, another 8 sample plots (1 in dolomite, 5 in limestone, and 2 in non-karst areas) in the areas with mature forests near Puding were investigated to estimate the maximum vegetation carbon density on each bedrock type.

Forest plots each with a projected area of 400 (20 $\times$ 20) m^2 were set for tree investigation, in which the species, diameter at breast height (DBH), and the height of woody and vine individuals with a DBH $\geq$ 3 cm were recorded to calculate the biomass of the tree layer. Then, 4 subplots each with an area of 25 m^2 were set for measuring the biomass of the shrub layer, in which the species, individual number, basal diameter, and the height of each woody plant with a DBH < 3 cm were recorded. As for grassland, 3 plots each

with an area of 1 m^2 were set for biomass estimation and the aboveground part of the grass in each plot was cut and weighed on site. Then about 1/10 samples were taken to the laboratory for water and carbon content measurement(the detailed investigation data is listed in File S3). The grass layer under each forest plot accounted for a very small proportion and, thus, its biomass was ignored. At the same time, the soil thickness of 3 plots on each of the vegetation types of grassland, shrubland, secondary forest, and primary forest on three main bedrock types had been measured. In each plot, soil thickness on at least 80 measure points with an interval of 1 m was measured by measuring rod; the total number of measure plots was 36.

2.3.2. Biomass and Carbon Calculation

The aboveground biomass of natural woody plants was calculated using the allometric equation of 15 dominant species established by Liu et al. [21] in an adjacent area. The belowground biomass of individuals with a DBH > 3 cm was calculated using the correlation equation between DBH and root biomass determined for main species in nearby karst habitats by Liu et al. [30]. The biomass of trees in plantations was calculated using the allometric equation constructed by Du et al. [31] for *Cunninghamia lanceolata* in a similar climatic zone. The belowground biomass of woody plants with a DBH < 3 cm, in either natural or plantation land, was determined by multiplying the corresponding aboveground biomass by 0.87, which is an overall biomass allocation coefficient between belowground and aboveground shrubs in China [32]. The aboveground biomass of herbaceous plants in grassland was gained from the plot measurements while the corresponding root biomass was computed by multiplying the aboveground biomass by 0.15 [33].

Then, vegetation carbon was determined by multiplying the biomass by the corresponding carbon contents of leaves and woods (0.479 and 0.482 $gC \cdot g^{-1}$, respectively) for natural woody plants [21]. As for artificial woody plants, the carbon contents were 0.4975 and 0.4753 $gC \cdot g^{-1}$, respectively, owing to the obvious species difference between natural and artificial vegetation. The carbon content of roots refers to that of branches. Finally, the carbon density of each plot was converted from its carbon storage and area. The carbon densities of dryland and paddy fields (3.889 and 7.378 $Mg \cdot ha^{-1}$, respectively) were cited from the vegetation carbon densities measured by Luo et al. [34]. The average carbon density of the plots with the same vegetation type was the estimated carbon density of this vegetation type. Then the carbon stock of each vegetation type was obtained by multiplying the carbon density by its area. The difference between the current vegetation carbon stock and the maximum vegetation carbon stock, which was replaced by the vegetation carbon stocks when all the artificial and natural forests reached the maximum vegetation carbon density of each bedrock, was taken as the vegetation carbon sequestration potential.

2.4. Data Analysis

One-way analysis of variance (ANOVA) was implemented with the shortest significant range at $p < 0.05$. Then, multiple comparisons were performed to test if there were significant differences in vegetation carbon density (VCD) among the three main bedrock types. The average soil thickness of all plots on the same bedrock types was used to evaluate the soil thickness of this bedrock type. To explore the relationships of vegetation carbon characteristics with human activity intensity and carbonate bedrock properties, we divided the study region by township areas into 11 parts. Then, the population density, area ratio of karst, area ratio of natural vegetation/plantation, average existing vegetation carbon density, and average vegetation carbon density growth potential in each part were statistically analyzed (File S1). After that, the correlation coefficient was calculated. These calculation processes were finished on SPSS PASW Statistics 18.

3. Results

3.1. Vegetation Distribution

Except for residential and industrial areas and water that were not concerned in this study, agricultural crops covered the largest area and exceeded 30% on all three bedrock types, in which the agricultural crops ratio was the largest in non-karst areas (40.01%) (Figure 3). Plantation and natural vegetation account for 25.6% and 28.12%, respectively, in non-karst areas, in which young plantation is the largest vegetation type with a ratio of 23.09%. The area ratios of shrub, shrub wood, and secondary forest are 9.25%, 9.68%, and 7.25%, respectively. Mature plantation covers only about 0.16% (Figure 3). In dolomite areas, grassland and shrubland, with area ratios of 16.12% and 15.77%, respectively, are the two most widespread types of natural vegetation. Plantation accounts for only 3.84% and there is nearly no mature plantation (0.12%) (Figure 3). In limestone areas, shrubland and shrub wood are the top two natural vegetation types, with area ratios of 16.93% and 19.24%, respectively. Grassland and plantation cover 10.33% and 8.46%, respectively (Figure 3). The mature forest cover just 0.16%, 0.24% and 0.34% of the areas on non-karst, limestone and dolomite, respectively. In the whole study region, the ratios of natural vegetation to plantation in non-carbonate, limestone, and dolomite areas are about 1.1, 6.44, and 11.67, respectively (Figure 3).

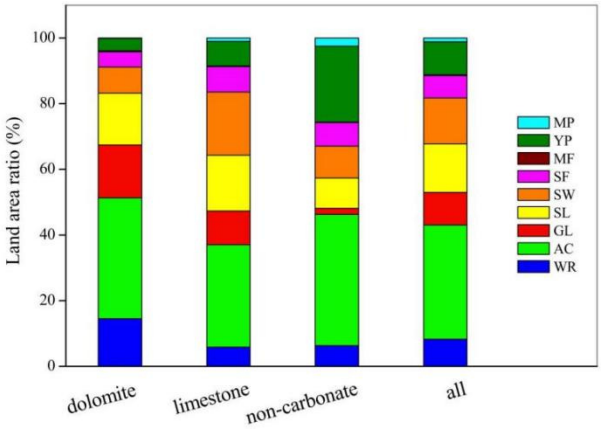


Figure 3. Land area ratios of vegetation types under the three bedrock types. WR: including water area (WA) and resident inhabitant area (RI). The vegetation carbon calculation in this study does not involve the WA and RI regions. Due to the lower vegetation carbon density (VCD) in these two regions, we have merged them into WR in this study.

In brief, the area ratios of grassland and shrubland in the karst areas are both obviously larger than in non-karst areas. However, the area ratio of plantations in non-karst areas is significantly higher than in karst areas. The ratio of shrub wood is the highest in the limestone area among the three bedrock types (Figure 3).

3.2. Existing Vegetation Carbon Density (VCD)

The average VCDs in the non-karst, limestone, and dolomite areas are 31.59 ± 7.43, 16.75 ± 4.12, and 8.26 ± 2.45 Mg·ha^{-1}, respectively (Figure 4). The average VCDs of plantations in the three bedrock areas are 73.20 ± 17.03, 49.92 ± 10.00, and 17.44 ± 11.32 Mg·ha^{-1}, respectively, with an average of 59.28 Mg·ha^{-1}. The average VCDs of natural vegetation are 30.62 ± 9.27, 17.68 ± 5.57, and 10.43 ± 3.70 Mg·ha^{-1}, respectively, with an average of 17.61 Mg·ha^{-1}. The average VCD of plantations is about 3.37 times that of natural vegetation. The VCDs are extremely low in the grass and shrub stages but grow quickly from shrubs to mature forests. In comparison, the VCDs of plantations on the three bedrock types can grow from 69.66, 45.99, and 16.05 Mg·ha^{-1} to 112.52, 84.09, and 64.24 Mg·ha^{-1}, respectively, when young plantations grow into mature plantations.

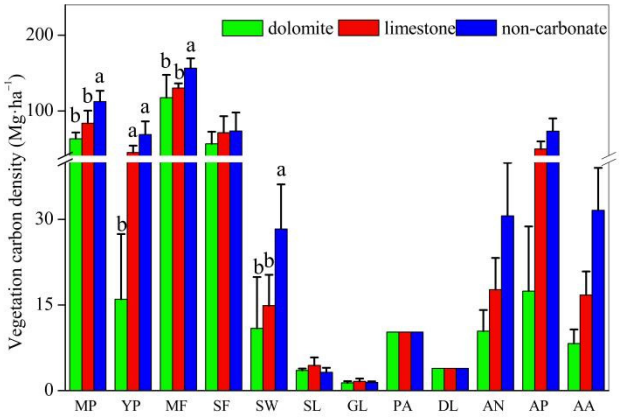


Figure 4. Vegetation carbon density (VCD) of each vegetation type under the three bedrock types. PA: paddy field, DL: dryland, AN: average VCD for natural vegetation, AP: average VCD for plantation, AA: average VCD for all vegetation types (including agricultural crops). The a and b for the same vegetation type indicate the carbon densities under different bedrock are significantly different at $p < 0.05$; multiple comparisons among three bedrocks had not been conducted for AN, AP, and AA.

The VCD in non-karst areas is the largest among the three bedrock types for almost all vegetation types, except secondary forests, and is significantly higher for shrub wood, mature forest, and plantation. The VCD in dolomite areas is always lower than compared with the other two bedrock types and is significantly lower for shrub wood, mature forest, and plantation. The maximum VCDs of natural vegetation on the three bedrock types are 156.49 ± 12.92, 130.27 ± 6.05, and 117.41 ± 30.03 Mg·ha^{-1}, respectively (Figure 4).

3.3. Existing Vegetation Carbon Stock and Sequestration Potential

3.3.1. Existing Vegetation Carbon Stock and Allocation

The vegetation carbon stocks in the dolomite, limestone, and non-karst areas are 208.49 ± 61.82, 855.69 ± 210.65, and 752.37 ± 172.85 Gg (10^9 g), respectively. The vegetation carbon stocks of secondary forest are the largest in both dolomite and limestone areas and are about 77.99 ± 21.97 and 300.64 ± 92.16 Gg, respectively. The dry land and shrub wood are also important vegetation carbon pools in dolomite areas and store about 37.20 and 25.65 ± 21.13 Gg, respectively. The young plantation contributes the least carbon (only 2.16 ± 0.28 Gg) to dolomite areas. In limestone areas, shrub wood and young plantation are the second and third contributors of vegetation carbon, respectively, and provide 155.64 ± 56.26 and 182.08 ± 36.51 Gg carbon, respectively. However, the grassland in limestone areas stores only about 9.15 ± 2.71 Gg vegetation carbon. In non-karst areas, the young plantation is the biggest vegetation carbon pool and its vegetation carbon stock is about 404.56 ± 101.53 Gg. The second to fourth vegetation carbon pools are secondary forest, shrub wood, and young plantation and provide 134.40 ± 44.47, 69.63 ± 49.24, and 71.53 ± 9.11 Gg carbon, respectively. Grassland is the smallest vegetation carbon contributor with a VCS of 0.67 ± 0.08 Gg (Figure 5).

In brief, young plantation and secondary forest are the two main vegetation carbon pools in this study region. Young plantation in non-karst areas provides the most vegetation carbon for plantation while the secondary forest on limestone contributes more vegetation carbon for natural vegetation.

The proportion of carbon in stems and branches increased with the evolution from natural shrubs into mature forests and from young plantations into mature plantations. The proportion of roots decreased in this process (the aboveground part of the grass was not separated). The leaf proportion remained the lowest and gradually declined in this process (except for mature forest on non-carbonate rocks) (Figure 6). The reason was that more biomass was injected into the stems and branches to compete for more sunlight (higher canopy) in the succession so that the proportions of leaves and roots were both lower. In

each plantation, the leaves of the young plantation on dolomite account for the highest proportion (Figure 6). Notably, the leaf proportion of mature forests is higher than in other stages of succession on non-carbonate rocks.

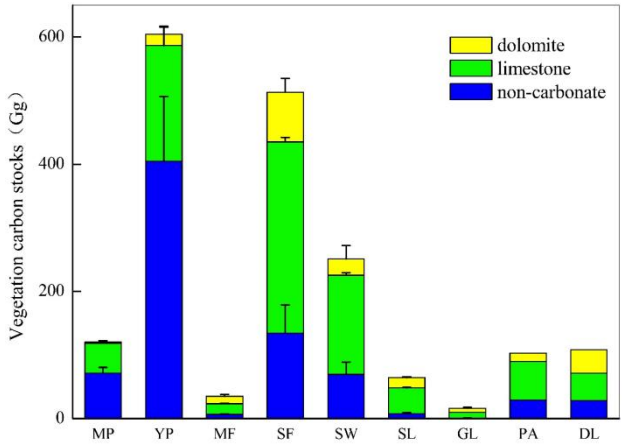


Figure 5. Vegetation carbon stocks of different vegetation types in areas of three bedrock types in Puding County.

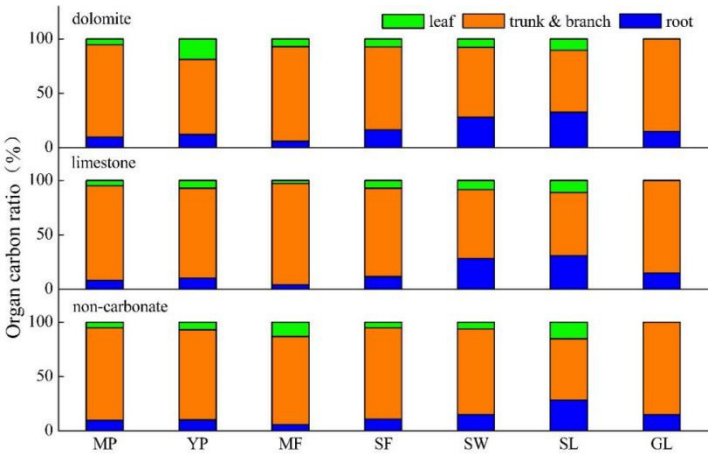


Figure 6. Allocation of vegetation carbon among organs under three bedrock types. The carbon amount of the leaves, trunks, and branches in grassland (GL) is considered to be the total value of the aboveground parts.

3.3.2. Vegetation Carbon Sequestration Potential

Under the promise that the area and VCD of agricultural crops remained unchanged, estimation showed the plantation and natural vegetation additionally fixed a total of about 6.06 Tg carbon. Specifically, the vegetation in non-carbonate, limestone, and dolomite areas fixed 1.15 ± 0.36, 3.44 ± 0.46, and 1.46 ± 0.47 Tg carbon, respectively, as plantations and natural vegetation continuously evolved into mature forests. The plantations on the three bedrock types sequestrated an additional 0.25, 0.16, and 0.05 Tg carbon, respectively (Figure 7B), which were equivalent to an increase in plantation VCD of 39.10, 33.83, and 45.89 $Mg \cdot ha^{-1}$, respectively (Figure 7A). In comparison, the natural vegetation on the three bedrock types sequestrated 0.89, 3.29, and 1.40 Tg carbon, respectively (Figure 7B), which were equal to VCD increases of ~120.17, 123.57, and 112.60 $Mg \cdot ha^{-1}$, respectively (Figure 7A). The VCD growth potentials of natural vegetation in non-carbonate, limestone, and dolomite areas reached 3.07, 3.65, and 2.45 times that of artificial forests, respectively (Figure 7A). The vegetation carbon stock growth potential of natural vegetation was 3.52, 21.16, and 26.97 times that of artificial forests, respectively, in the study area (Figure 7B).

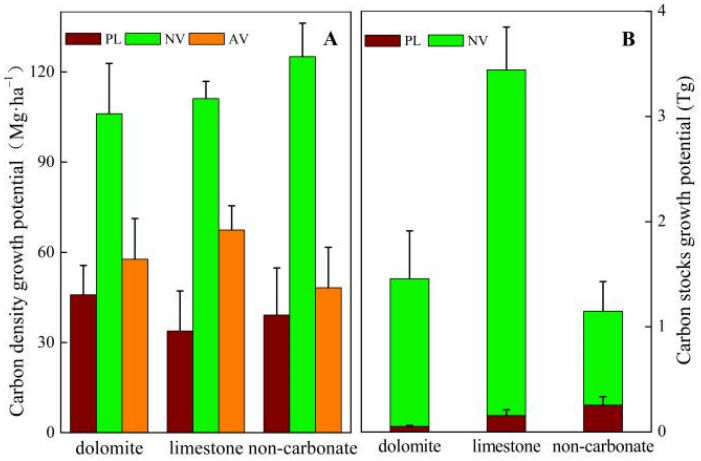


Figure 7. Growth potential of vegetation carbon density (**A**) and stocks (**B**) under the three bedrock types. NV: natural vegetation, PL: plantation, AV: average value (including agricultural crops).

4. Discussion

4.1. The Vegetation Carbon Characteristics on the Three Main Bedrocks

The results above indicate the existing VCD and MVCD are both the highest on non-carbonate rocks and the lowest on dolomite. The MVCDs on all three bedrock types are lower than the average vegetation carbon capacity of subtropical evergreen broad-leaved forests in China (167.4 ± 58.6 Mg·ha^{-1}) [22]. The MVCD on non-carbonate rocks is higher than that of mature forests in China (129.26 Mg·ha^{-1}) and the average aboveground VCD of primary forests in Houzhai watershed, Southwest China (142.2 Mg·ha^{-1}) [20,23]. The existing VCDs on the two carbonate rock areas are both significantly lower than that on non-carbonate rocks and are both lower than the average VCD of forests in Guizhou (27.886 Mg·ha^{-1} [35]) and forests in China (69.23 Mg·ha^{-1}) [23]. The existing VCD of plantations (59.28 Mg·ha^{-1}) is higher than that of natural vegetation and the average VCD of a Chinese fir plantation (47.6 Mg·ha^{-1}) in nearby Hubei Province [36]. The vegetation carbon sequestration potential of the study region accounts for only about 0.05% of the increase in vegetation carbon storage potential in China (10.81 Pg) [23].

The root proportion of vegetation in non-karst bedrock areas is smaller compared to vegetation on karst bedrock, which is consistent with previous research [37]. The root proportion of vegetation on dolomite is slightly higher than that on limestone. The reason is that the soil on dolomite has a lower soil water-holding capacity than that on limestone due to its shallower and more even soil layer [38] and, thus, more biomass is invested in roots to absorb more water in this environment. The sudden rise in the leaf ratio on non-carbonate rocks when secondary forests evolve into mature forests can be explained by the fact that the dominant species of the tree layer change from deciduous to evergreen trees in this process and evergreen species have a higher leaf proportion than deciduous species [39].

4.2. Bedrock Effects on Vegetation Carbon (Natural Processes)

The above results imply that the underlying bedrocks greatly influence both the existing VCD and the MVCD in the study region. The thicker soil and higher bedrock exposure rate may limit the MVCD in carbonate rocks (Figure 8). The low acid-insoluble content in carbonate rocks causes a slower soil formation process [11]. In addition, the porous karst bedrock and abundant rainfall accelerate soil erosion. All of these changes lead to a lower soil amount in karst areas. At the same time, the high pH may reduce the activities of some mineral nutrients (e.g., phosphorus) in the soil, resulting in physiological stress [28]. The higher calcium and magnesium contents may intensify this stress. The lower soil amount also results in a low water storage capacity as the soil can only supply water for 7–10 days to its overlying vegetation, even in the case of full water [14]. The

harsh karst environment not only creates significant differences in species composition between karst vegetation and non-karst vegetation [40] but also slows down the growth of karst vegetation and leads to lower maximum biomass [16,18]. All of these stresses lead to significantly smaller proportions of grasslands, shrubs, and shrub wood in non-karst areas than in karst areas (Figure 3) and, in turn, cause a lower existing VCD on karst than on non-carbonate bedrocks. This result indicates bedrocks can impact the existing VCD, the MVCD, and the carbon allocation by affecting soil properties. Furthermore, the precipitation may decrease in the mid-latitude regions of the northern hemisphere [41], which may exacerbate the drought stress on karst vegetation, especially vegetation on dolomite, and enlarge the VCD difference between vegetation on karst and non-carbonate rock.

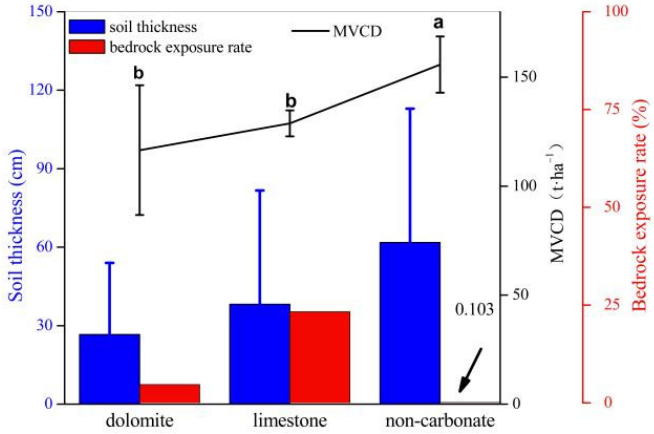


Figure 8. Relationships between vegetation carbon density of mature forests and soil thickness or bedrock exposure rates under the three bedrock types. MVCD: maximum vegetation carbon densities of natural vegetation.The a and b for the MVCD indicate the maximum carbon densities under different bedrock are significantly different at $p < 0.05$.

4.3. Bedrock Effects on Vegetation Carbon Through Human Activities

Vegetation can be affected by human activities in two opposite ways: destruction and protection or reconstruction. However, the orientation and intensity of human activities are influenced by the natural background, such as soil characteristics, topography, and geomorphology, which are greatly controlled by the bedrocks.

On the one hand, bedrocks may impact the VCD by affecting the damage activity of humans. Human activities (e.g., cultivation, grazing, and logging) are the basic activities to ensure the normal production and life of people in mountainous areas. These activities will damage vegetation and excessive and unreasonable activities can even lead to serious ecological problems, such as rocky desertification in karst areas [10]. However, as a result of the conscious and selective utilization by humans, the type and intensity of human activities differ among areas with different environments. For example, people tend to cultivate in small-slope areas because of easier cultivation and more fertile soil. Consequently, population density in the small-slope areas may increase, causing more damage. However, the slope is impacted by the bedrock type. Our analysis of the slope map of the study region shows the area proportions of slopes $\leq 25^{\circ}$ (the maximum slope allowed for cultivation by Chinese laws) in dolomite and limestone areas are 84.85% and 77.79%, respectively, which are both slightly higher than that of non-carbonate rock areas (76.84%). Hence, human activities, which affect the vegetation, are influenced by bedrocks. The above results may elucidate the opposite correlation between the existing VCD and the karst area ratio (Table 1). In addition, the higher bedrock exposure rate may limit the plant density in plantations, which is the main carbon contributor to the existing VCD and, thereby, reduces the existing VCD.

Table 1. Correlation coefficients between vegetation carbon and influence factors.

Factors	ECD	CDGP	PD	RK	RP	RN
ECD	1.000					
CDGP	0.823 **	1.000				
PD	−0.803 **	−0.867 **	1.000			
RK	−0.773 **	−0.623 *	0.507	1.000		
RP	0.905 **	0.680 *	−0.605 *	−0.651 *	1.000	
RN	0.194	0.653 *	−0.583 *	−0.074	−0.082	1.000

Note: ECD: Existing vegetation carbon density, CDGP: Vegetation carbon density growth potential, PD: Population density, RK: Area ratio of karst, RP: Area ratio of plantation, RN: Area ratio of natural vegetation. The population density of each town was obtained by dividing the population by its area. Population data were cited from the Seventh Population Census of China. ** indicates a very significant correlation at the confidence level of $p < 0.01$. * indicates a significant correlation at the confidence level of $p < 0.05$.

On the other hand, the bedrock types may impact the existing VCD and the growth potential of the VCD by adjusting the area ratio of the plantations on each bedrock type. Plantations are one important way of vegetation reconstruction [42]. In this study, the area proportions of plantations to natural vegetation in non-carbonate, limestone, and dolomite areas are about 0.91, 0.16, and 0.09, respectively (Figure 3). Moreover, the average existing VCDs of plantations are about 2.39, 2.88, and 1.67 times those of natural vegetation, respectively. The higher plantation ratio in non-carbonate areas will increase the existing VCD. This inference is supported by the large opposite relationship between the existing VCD and the ratio of plantations. Despite the higher existing VCD of plantations, the vegetation carbon sequestration potential of plantations is significantly lower than that of natural vegetation, owing to the quick growth of plantations in the early stage. Therefore, the higher proportion of plantations in non-carbonate areas will lead to a lower vegetation carbon sequestration potential. The growth potential of VCD is positively correlated with the proportion of natural vegetation (Table 1). The proportion of plantations is controlled by the conscious selection of human activities that are strongly influenced by soil properties, which are greatly determined by the bedrock type. Hence, the bedrock type significantly impacts the existing VCD and vegetation carbon sequestration potential. Clearly, plantation provides more carbon accumulation for vegetation but natural vegetation will become the main contributor to vegetation carbon sequestration in the subsequent succession, especially in karst areas. Thereby, the best way to sequestrate more vegetation carbon is natural recovery through eco-engineering and rural out-migration, which can both generate great carbon sinks [26,43].

However, karst ecosystems are complex so accurate estimation of vegetation carbon in these systems is still difficult. Although we obtained the vegetation map of Puding County by combining sample surveys with ArcGIS, there are many other types of landforms in karst areas [44]. Further investigations are needed to clarify whether our results are applicable if we expand from the sample scale to the regional scale. Therefore, we still need more empirical means combined with observation equipment to make a more accurate estimation.

5. Conclusions

Through a number of sample surveys and a detailed vegetation map, we statistically calculated the existing vegetation carbon density and the carbon stock and carbon sequestration potential in typical karst areas and analyzed the impacts of bedrock types on vegetation carbon. The existing vegetation carbon density in non-carbonate rock areas is higher than that in karst areas, especially in shrub forests, mature forests, and artificial forests. However, the vegetation in karst areas has a higher potential to increase carbon density compared with that in non-karst areas. The bedrock type can strongly impact the accumulation rate and sequestration potential of vegetation carbon in the study region directly by influencing the vegetation growth environment and indirectly by influencing human activities. Plantations positively affect vegetation carbon accumulation in the early

stage of vegetation restoration but natural vegetation has a greater carbon sequestration potential in the later vegetation succession. Natural restoration is the best way to increase carbon accumulation in karst ecosystems.

Supplementary Materials: The following supporting information can be downloaded at: https://www.mdpi.com/article/10.3390/su16219429/s1, File S1: Township level data of a part of factors that may influence the carbon density; File S2: Attribute table of vegetation map; File S3: Plots survey data.

Author Contributions: Conceptualization, C.L.; data curation, C.L. and Z.H.; formal analysis, X.C.; funding acquisition, W.L., C.L., J.C., and S.W.; investigation, X.C., C.L., and Z.H.; methodology, X.C., C.L., and Z.H.; project administration, C.L.; resources, W.L., C.L., and S.W.; validation, X.C. and Z.H.; writing—original draft, X.C.; writing—review and editing, W.L., C.L., J.C., L.Z., and A.C. All authors have read and agreed to the published version of the manuscript.

Funding: This research was funded by the Strategic Priority Research Program of the Chinese Academy of Sciences, grant number XDB40020200; the National Natural Science Foundation of China, grant numbers 42273021 and U2244216; the China Postdoctoral Science Foundation, grant number 2021M703187; and the Guizhou Provincial Science and Technology Projects, grant number Qiankehejichu-ZK [2022]Yiban564.

Institutional Review Board Statement: Not applicable.

Informed Consent Statement: Not applicable.

Data Availability Statement: The data presented in this study are available on request from the corresponding author.

Acknowledgments: We sincerely thank the anonymous reviewers and editors for their valuable comments and suggestions. We sincerely thank all the people who provided help to us during our study and paper writing.

Conflicts of Interest: The authors declare no conflict of interest.

References

1. Myneni, R.; Dong, J.; Tucker, C.; Kaufmann, R.K.; Kauppi, P.E.; Liski, J.; Zhou, L.; Alexeyev, V.; Hughes, M.K. A large carbon sink in the woody biomass of Northern forests. *Proc. Natl. Acad. Sci. USA* **2001**, *98*, 14784–14789. [CrossRef] [PubMed]
2. Yadvinder, M.; Meir, P.; Brown, S. Forests, carbon and global climate. *Philos. Trans. Math. Phys. Eng. Sci.* **2002**, *360*, 1567–1591.
3. Li, P.; Zhu, J.; Hu, H.; Guo, Z.; Pan, Y.; Birdsey, R.; Fang, J. The relative contributions of forest growth and areal expansion to forest biomass carbon sinks in China. *Biogeosci. Discuss.* **2015**, *12*, 9587–9612.
4. Zhang, C.; Xiao, Q.; Wu, Z.; Martin, K. Ecosystem-driven karst carbon cycle and carbon sink effects. *J. Groundw. Sci. Eng.* **2022**, *10*, 99–112.
5. Ministry of Ecology and Environment of China. Available online: https://www.mee.gov.cn/xxgk/hjyw/202312/t20231229_1060290.shtml (accessed on 30 December 2023).
6. Wen, D.; He, N. Forest carbon storage along the north-south transect of eastern China: Spatial patterns, allocation, and influencing factors. *Ecol. Indic. Integr. Monit. Assess. Manag.* **2016**, *61*, 961–967. [CrossRef]
7. Fan, J.; Zhong, H.; Harris, W.; Yu, G.; Wang, S.; Hu, Z.; Yue, Y. Carbon storage in the grasslands of China based on field measurements of above- and below-ground biomass. *Clim. Chang.* **2008**, *86*, 375–396. [CrossRef]
8. Guo, Z.; Pan, Y.; Richard, B. Inventory-based estimates of forest biomass carbon stocks in China: A comparison of three methods. *For. Ecol. Manag.* **2010**, *259*, 1225–1231. [CrossRef]
9. Jiang, Z.; Liu, H.; Wang, H.; Peng, J.; Meersmans, J.; Green, S.M.; Quine, T.A.; Wu, X.; Song, Z. Bedrock geochemistry influences vegetation growth by regulating the regolith water holding capacity. *Nat. Commun.* **2020**, *11*, 2392. [CrossRef]
10. Wang, S. The Most Serious Eco-geologically environmental Problem in Southwestern China—Karst Rocky Desertification. *Bull. Mineral. Petrol. Geochem.* **2003**, *22*, 120–126.
11. Wang, S.; Ji, H.; Ouyang, Z. A preliminary study on the weathering of carbonate rocks. *Sci. China (Ser. D)* **1999**, *29*, 441–449.
12. Yuan, D. On the karst ecosystem. *Acta Ecol. Sin.* **2001**, *75*, 336–338.
13. Cao, J.; Yuan, D.; Tong, L. Features of karst ecosystem and intergrating maesure for karst desertification in southwest China. *Pratacult. Sci.* **2008**, *25*, 40–50.

14. Zhou, Y.; Pan, G. Adaptation and adjustment of Maolan forest ecosystem to karst environment. *Carsologica Sin.* **2001**, *20*, 47–52.
15. Zhang, X.; Wang, K. Ponderation on the shortage of mineral nutrients in the soil-vegetation ecosystem in carbonaterock-distributed mountain regions in Southwest China. *Earth Environ.* **2009**, *37*, 337–341.
16. Ni, J.; Xu, H.; Liu, L. Low net primary productivity of dominant tree species in a karst forest, southwestern China: First evidences from tree ring width and girth increment. *Acta Geochim.* **2017**, *36*, 482–485. [CrossRef]
17. Yang, H.; Cheng, S. Study on biomass of the karst forest community in Maolan, Guizhou Province. *Acta Ecol. Sin.* **1991**, *11*, 307–313.
18. Zhu, S.; Wei, L.; Chen, Z.; Zhang, C. A preliminary study on biomass components of karst forest in Maolan of Guizhou Province, China. *Acta Phytoecol. Sin.* **1995**, *19*, 358–367.
19. Huang, Z.; Yu, L.; Fu, Y.H. Characteristics of carbon sequestration during natural restoration of Maolan karst forest ecosystems. *Chin. J. Plant Ecol.* **2015**, *39*, 554–564.
20. Liu, C.; Liu, Y.; Guo, K.; Wang, S.; Liu, H.; Zhao, H.; Qiao, X.; Hou, D.; Li, S. Aboveground carbon stock, allocation and sequestration potential during vegetation recovery in the karst region of southwestern China: A case study at a watershed scale. *Agric. Ecosyst. Environ.* **2016**, *235*, 91–100. [CrossRef]
21. Liu, Y.; Liu, C.; Wang, S.; Guo, K.; Yang, J.; Zhang, X.; Li, G. Organic Carbon Storage in Four Ecosystem Types in the Karst Region of Southwestern China. *PLoS ONE* **2013**, *8*, e56443. [CrossRef]
22. Liu, Y.; Yu, G.; Wang, Q.; Zhang, Y.; Xu, Z. Carbon carry capacity and carbon sequestration potential in China based on an integrated analysis of mature forest biomass. *Sci. China-Life Sci.* **2014**, *57*, 1218–1229. [CrossRef] [PubMed]
23. Li, X.; Wen, D.; Zhu, J.; He, N. Regional Variation in Carbon Sequestration Potential of Forest Ecosystems in China. *Chin. Geogr. Sci.* **2017**, *27*, 337–350.
24. Chen, C.; Park, T.; Wang, X.; Piao, S.; Xu, B.; Chaturvedi, R.K.; Fuchs, R.; Brovkin, V.; Ciais, P.; Myneni, R.B.; et al. China and India lead in greening of the world through land-use management. *Nat. Sustain.* **2019**, *2*, 122–129. [CrossRef]
25. Tong, X.; Brandt, M.; Yue, Y.; Horion, S.; Wang, K.; Keersmaecker, W.D.; Tian, F.; Schurgers, G.; Xiao, X.; Fensholt, R.; et al. Increased vegetation growth and carbon stock in China karst via ecological engineering. *Nat. Sustain.* **2018**, *1*, 44–50. [CrossRef]
26. Chang, J.; Yue, Y.; Tong, X.; Brandt, M.; Zhang, C.; Zhang, X.; Qi, X.; Wang, K. Rural outmigration generates a carbon sink in South China karst. *Prog. Phys. Geogr. Earth Environ.* **2023**, *47*, 655–667. [CrossRef]
27. Sun, C.; Wang, S.; Zhou, D.; Li, R.; Li, Y. Differential weathering and pedogentic characteristics of carbonate rocks and their effect on the development of rock desertification in karst regions. *Acta Mineral. Sin.* **2002**, *22*, 308–314.
28. Liu, C. *Biogeochemical Processes and Cycling of Nutrients in the Earth's Surface: Cycling of Nutrients in Soil-Plant Systems of Karstic Environments, Southwest China*; Science Press: Beijing, China, 2009; pp. 401–439.
29. Yu, L.; Zhu, S.; Wei, L.; Chen, Z.; Xiong, Z. Study on the natural restoration process of degraded karst communities successional sere. *Mt. Agric. Biol.* **1998**, *17*, 71–77.
30. Liu, L.; Zhong, Q.; Ni, J. Allometric function based root biomass estimate of woody plants in a karst evergreen and deciduous broad-leaf mixed forest in central Guizhou Province, Southwestern China. *Acta Ecol. Sin.* **2018**, *38*, 8726–8732.
31. Du, H.; Zeng, F.; Wang, K.; Song, T.Q.; Wen, Y.G.; Li, C.G.; Peng, W.X.; Liang, H.W.; Zhu, H.G.; Zeng, Z.X. Dynamics of biomass and productivity of three major plantation types in southern China. *Acta Ecol. Sin.* **2014**, *34*, 2712–2724.
32. Wang, Y. Biomass Allocation and Spatial Distribution in Shrubland Ecosystems in China. Ph.D. Thesis, University of Chinese Academy of Sciences, Beijing, China, 12 July 2018.
33. Ma, A.; Yu, G.; He, N.; Wang, Q.; Peng, S. Above- and below-ground biomass relationships in China's grassland vegetation. *Quat. Sci.* **2014**, *34*, 769–776.
34. Luo, H.; Yuan, D.; Chen, H. Organic carbon density of farmland ecosystem in karst area of Sanquan town, Nanchuan city. *Carsologica Sin.* **2008**, *27*, 382–387.
35. Guo, C.; Wu, Y.; Ni, J.; Guo, Y. Forest carbon storage in Guizhou Province based on field measurement dataset. *Acta Geochim.* **2019**, *38*, 8–21. [CrossRef]
36. Ma, Y. Characteristics and Distributions of Biomass and Carbon Storage of Chinese Fir Plantation in Hubei Province. Master's Thesis, Central South University of Forestry and Technology, Changsha, China, 2023.
37. Ni, J.; Luo, D.; Xia, J.; Zhang, Z.H.; Hu, G. Vegetation in karst terrain of southwestern China allocates more biomass to roots. *Solid Earth* **2015**, *6*, 799–810. [CrossRef]
38. Jia, Z.; Yu, L.F. Soil properties and correlation analysis on karst rocky desertification area of limestone and dolomite. *Chin. J. Guizhou Sci.* **2010**, *28*, 29–33.
39. Nagayama, Y.; Li, C.; Katagiri, S. Above-ground Biomass, Net Primary Production, Nutrient Distribution and Nutrient Use Efficiency in Natural Evergreen Broad-leaved Forest in Southern China. *Jiangxi For. Sci. Technol.* **2005**, *S1*, 17–24.
40. Liu, Y.; Liu, C.; Matteo, R. An Assessment of Soil's Nutrient Deficiencies and Their Influence on the Restoration of Degraded Karst Vegetation in Southwest China. *Forests* **2020**, *11*, 797. [CrossRef]
41. John, F.; Mitchell, B. The "Greenhouse" effect and climate change. *Rev. Geophys.* **1989**, *27*, 115–139.
42. Gao, L.; Li, H. Improving Carbon Sequestration Capacity of Forest Vegetation in China: Afforestation or Forest Management? *Forests* **2023**, *14*, 1077. [CrossRef]

43. Zhang, X.; Yue, Y.; Tong, X.; Wang, K.; Qi, X.; Deng, C.; Brandt, M. Eco-engineering controls vegetation trends in southwest China karst. *Sci. Total Environ.* **2021**, *770*, 145–160. [CrossRef]
44. Wang, S.; Zhang, X.; Bai, X. An Outline of Karst Geomorphology Zoning in the Karst Areas of Southern China. *Chin. J. Mt. Res.* **2015**, *33*, 641–648.

Disclaimer/Publisher's Note: The statements, opinions and data contained in all publications are solely those of the individual author(s) and contributor(s) and not of MDPI and/or the editor(s). MDPI and/or the editor(s) disclaim responsibility for any injury to people or property resulting from any ideas, methods, instructions or products referred to in the content.